International Journal of
Automotive Manufacturing and Materials (IJAMM)

Scilight

Article

Exhaust Noise Optimization of Gas Engine Aftertreatment

Miaomiao Chen *, Chenghui Xu, Juan Li, Wenran Zhao, Pengyuan Li, Zhen Chen, Jia Zhang, and Lei Zhang

Dongfeng Commercial Vehicle Technical Center, Dongfeng Commercial Vehicle Co., Ltd., Wuhan 430057, China
* Correspondence: chenmiaomiao@dfcv.com.cn
Received: 23 September 2025; Revised: 15 December 2025; Accepted: 22 December 2025; Published: 5 February 2025

Abstract: To address exhaust noise from gas engines in commercial vehicles without altering the existing aftertreatment system layout, two muffler optimization strategies were investigated. Scheme 1 involved adding a perforated baffle, while Scheme 2 further optimized the perforated inlet pipe based on Scheme 1. The noise reduction performance was evaluated through acoustic simulation (insertion loss) and vehicle testing (pass-by noise). Compared with Scheme 1, Scheme 2 demonstrated superior noise performance, achieving insertion loss improvements of 4.2 dB and 1.8 dB at 600 rpm and 1800 rpm, respectively. At 600 rpm, test results indicated that both schemes were insensitive to 3rd- and 9th-order noise, indicating limited effectiveness of structure-based interventions under low-speed conditions. When the operating speed increased to 650 rpm, Scheme 2 reduced 3rd-order noise by 8.00 dB through pre-control of the flow field. This study demonstrates the effectiveness of combined perforated baffle and inlet pipe optimization under fixed structural constraints and provides a technical reference for noise control in gas engine aftertreatment systems and muffler design in similar applications.

Keywords: muffler optimization; exhaust noise reduction; insertion loss; order noise

1. Introduction

The increasing adoption of natural gas commercial vehicles, driven by energy-efficiency and emission-reduction policies, has intensified the focus on the acoustic performance of exhaust aftertreatment systems. Exhaust noise significantly influences overall noise, vibration, and harshness (NVH) performance of a vehicle and strongly affects driver perception. It is considered equally important to power performance, safety, and reliability. Given the stringent layout constraints of the aftertreatment systems and the requirement to maintain emission control efficiency, developing cost-effective exhaust noise-reduction solutions has become a persistent engineering challenge.

Research on muffler acoustics has advanced through theoretical investigations, structural design studies, and engineering validation. Munjal [1] systematically reviewed the recent developments in muffler acoustic design, emphasizing the influence of cavity volume, perforation impedance, and flow-related effects on insertion loss. Bire and Shelke [2] achieved targeted attenuation of order noise under space-constrained conditions, with optimized internal structures incorporating small-volume cavities and resonant membrane-based pressure-wave absorption. From an engineering perspective, Kashikar et al. [3] demonstrated that practical modifications to internal configurations can improve insertion loss while maintaining acceptable backpressure. Experimental work by Sedighi et al. [4] further confirmed that structural refinements can effectively suppress exhaust noise and enhance sound quality in small engines.

Multidisciplinary design approaches have proven effective in vibration and noise control across various engineering fields [5–7]. Parameter-driven studies have provided quantitative insights into internal geometry. Mohammad et al. [8] showed that cavity volume, pipe diameter, and perforation ratio strongly affect both insertion loss and pressure drop. Optimization-oriented approaches, such as the finite-element–Kriging–multiobjective framework used by Li et al. [9], revealed that combining perforated tubes with parallel chambers can simultaneously enhance acoustic attenuation and reduce pressure loss. Structural improvements, including the integration of baffle plates, have been reported to increase insertion loss by approximately 10% [10]. In addition, acoustic–structure coupling analyses demonstrated that elastic deformation can significantly shift insertion loss peaks [11].

Despite significant advancements in muffler design, a major challenge persists in achieving a balance of layout, structure and cost under engineering applications. Specifically, the influence of internally redesigned mufflers constrained by existing aftertreatment housing dimensions on vehicle pass-by noise and order-based noise characteristics has not been sufficiently investigated. Thus, two muffler optimization schemes are proposed based on the existing structure. A comprehensive comparison of the three structures was unavailable. The present study comparatively investigates insertion loss through simulation and the pass-by noise through experimental testing. Moreover, the 3rd-, 6th-, and 9th-order noise components at different engine speeds are analyzed to clarify the underlying noise control mechanisms.

2. Optimization Strategy

2.1. Structural Design of Optimization

Considering comprehensive factors such as design cost, R&D cycle, and verification cycle, the muffler optimization strategy focuses on modifying specific components of the muffler structure while maintaining the existing aftertreatment system dimensions and three-way catalytic converter layout [12]. These modifications are expected to further enhance the insertion loss of the aftertreatment system across the entire exhaust path, thereby improving its acoustic attenuation performance. The optimization directions are determined as follows:

Scheme 1: Add a layer of perforated baffles to attenuate noise through absorption and reflection of sound waves.

Scheme 2: Enhance the flow of exhaust gases by incorporating a perforated structure into the inlet pipe to reduce low-frequency intake noise.

The proposed aftertreatment system improvement schemes, along with the corresponding schematic diagrams of the muffler structural modifications, are presented in Table 1 and Figure 1.

Table 1. Aftertreatment System Improvement Schemes.

Scheme	Number of Perforated Baffles	Perforated Pipe at Inlet
Original Scheme	2	No
Scheme 1	3	No
Scheme 2	3	Yes

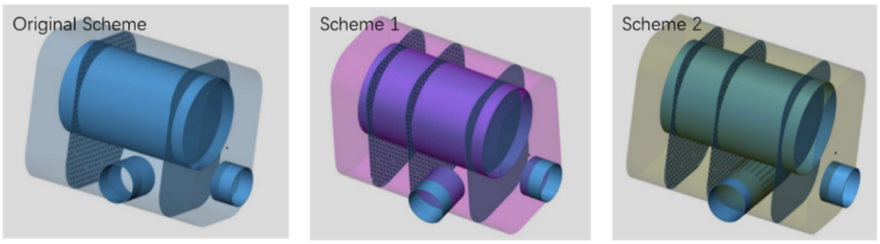

Figure 1. Schematic Diagrams of the Muffler Structural Modifications.

2.2. Acoustic Performance Evaluation metrics

2.2.1. Insertion Loss

Insertion loss (*IL*) is a key performance indicator used to evaluate the acoustic performance of the aftertreatment system. It is defined as "the difference in the sound pressure level at the exhaust outlet with and without the aftertreatment system under identical engine operating conditions [13]. *IL* reflects the change in acoustic performance of a noise-reduction structure before and after its integration into the aftertreatment system. Therefore, it directly indicates the noise-control capability of the structure, and a larger *IL* value corresponds to stronger noise-reduction effect.

$$IL = L_{P'} - L_P = 20lg(P'/P) \quad (1)$$

The *IL* calculation involves several parameters. Specifically, IL represents the insertion loss; $L_{P'}$ represents the sound pressure level at the exhaust outlet without the aftertreatment system; and L_P represents the sound pressure level of the exhaust outlet with the system installed. Similarly, P' and P correspond to the sound pressure level of the exhaust outlet without and with the aftertreatment system, respectively, under comparable operating conditions.

2.2.2. Order Noise

To characterize the order-related features of exhaust noise, engine order noise is adopted as an important performance metric in this study. The fundamental frequency of engine exhaust noise is determined by [14]:

$$f = n \times z/(60 \times i) \quad (2)$$

where n represents the engine speed, z denotes the number of cylinders, and i corresponds to half of the engine stroke cycle. As indicated by Equation (2), exhaust noise contains a fundamental frequency component associated with periodic engine excitation, as well as a series of higher-order harmonics whose frequencies correspond to integer multiples of the fundamental excitation.

For four-stroke, six-cylinder engines, the 3rd-, 6th- and 9th order noise are directly associated with the primary excitation sources and account for a substantial proportion of the acoustic energy. These three orders are also more likely to couple with structural resonances, thereby exerting a notable impact on acoustic performance under practical operating conditions. Therefore, the 3rd-, 6th- and 9th-order noise engine orders are selected as the principal indicators for order-based acoustic evaluation.

2.2.3. Vehicle Pass-by Noise

Vehicle pass-by noise refers to the noise radiated by a vehicle as it passes a fixed observation point under specified operating conditions. It represents the overall noise emission at the vehicle level, incorporating the combined effects of exhaust radiation, powertrain excitation, and vehicle installation characteristics.

In this study, vehicle pass-by noise is adopted as the final vehicle-level evaluation metric, and the corresponding test results serve as the ultimate criterion for assessing the effectiveness of the proposed optimization schemes under realistic operating conditions.

3. Numerical and Experimental Methods

3.1. Simulation Methods

To quantitatively evaluate the acoustic performance of the baseline and optimized aftertreatment schemes, three-dimensional geometry of each scheme was first created in GEM3D (v2016) and then converted into an equivalent one-dimensional acoustic network models through the standard discretization procedure in GT-Power (v2016). This procedure uses the internal component library and segmentation rules to assign pipe elements, volumes, and acoustic properties, ensuring consistent modeling across different schemes.

For acoustic analysis, a coupled one-dimensional engine–aftertreatment model was established, as shown in Figure 2. The engine model was a calibrated GT-Power model whose key performance parameters were adjusted according to dynamometer measurements. The calibrated model provides realistic exhaust boundary conditions, including mass flow rate, temperature, and pressure pulsation, which are essential for predicting the system-level acoustic response. The inlet of the aftertreatment system was directly coupled to the calibrated engine model, and the outlet was specified as an open termination. The insertion loss of each scheme was obtained by comparing the exhaust outlet sound pressure levels with and without the aftertreatment system installed. Using insertion loss as the primary evaluation metric, the acoustic performance of the optimized schemes was systematically compared with that of the baseline scheme.

3.2. Experiment Methods

The vehicle pass-by noise measurements were conducted in accordance with GB/T 14365, Acoustics-Measurement Method for Sound Pressure Level of Stationary Noise of Motor Vehicles. The ambient temperature during the test was controlled within the range of −5 °C to 40 °C, and the wind speed at the height of the microphone did not exceed 5 m/s. A wind deflector was installed when the wind speed exceeded 2 m/s to prevent exhaust wake interference, ensuring the test results were not influenced by gusts. The test site was selected as an open and flat area, with no large sound reflectors within a radius of 10 m centered on the vehicle, and the ground was hard-paved to ensure acoustic consistency. A sound pressure level meter and a multi-channel data acquisition system meeting the requirements of GB/T 3785.1 were employed for exhaust noise measurement. The auxiliary measuring point of exhaust noise was 0.5 m away from the exhaust outlet and oriented 45° relative to the exhaust flow direction (0.3 m from the ground), while avoiding direct exposure to the exhaust jet, as shown in Figure 3. The uniformity of the sound field was required to satisfy the condition that the sound pressure level deviation over the hemispherical surface in all directions remained within ±1 dB when a non-directional small sound source was placed in the center of the site. No shelter was permitted within 1 m of the microphone. During the measurements, personnel were prohibited from

standing between the sound source and the microphone to avoid disturbing the sound field. Before the test, the vehicle underwent a warm-up process during which the coolant temperature was required to reach at least 80 °C. After the engine was started, the vehicle was maintained at idle speed for 30 s. Once the engine reached stable operating conditions, data collection was initiated, and the sound pressure signals were continuously recorded for 10 s. A measurement was considered valid when the deviation among the three test results was less than 0.5 dB (A). The arithmetic mean of the valid measurements was then reported as the final test result.

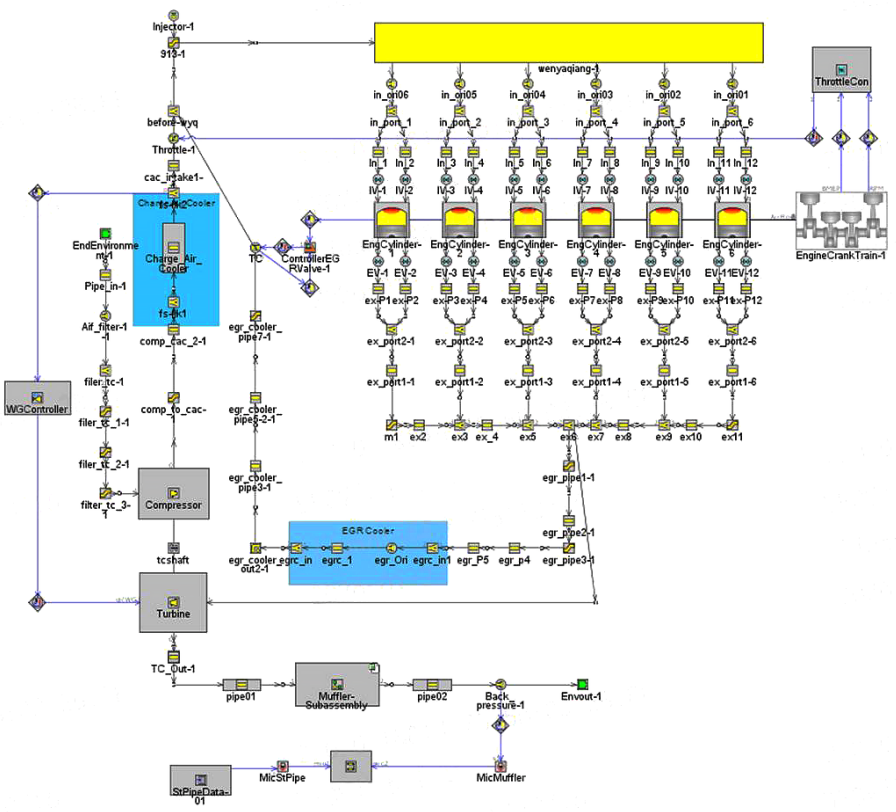

Figure 2. Model for post-processing insertion loss.

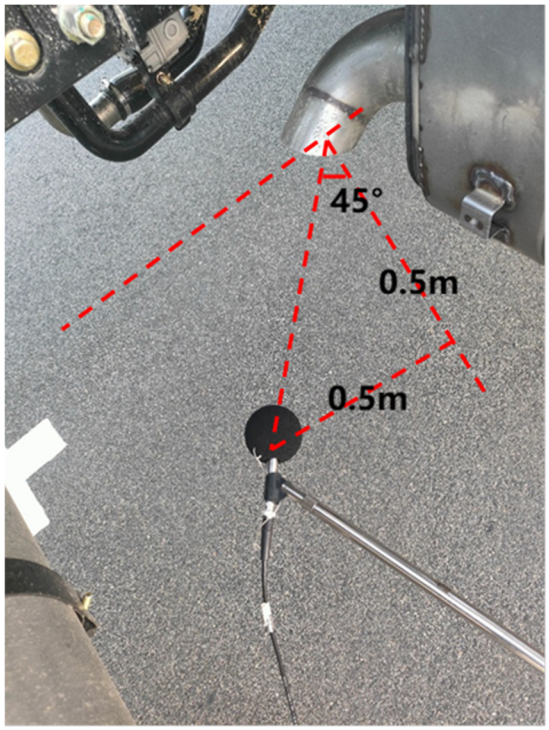

Figure 3. Layout of exhaust noise measurement point.

4. Results and Discussion

4.1. Simulation Results and Discussion

Figure 4 shows the insertion loss corresponding to different aftertreatment muffler schemes at the engine speed of 600 rpm. In Scheme 1, the addition of a perforated baffle reduces medium and high frequency acoustic energy through resonance scattering, increasing the insertion loss for the 6th-order noise by 3.5 dB. Scheme 2 further incorporates a perforated structure in the inlet pipe, which integrates flow disturbance with acoustic impedance regulation. Leveraging the Bernoulli effect, it alters the flow-field parameters, thereby promoting noise interference cancellation. Simultaneously, the transmission and absorption of acoustic energy are optimized. This optimization attenuates the 3rd-order noise by 4.6 dB and the 6th-order by 7.9 dB. Ultimately, the total insertion loss is enhanced by 4.2 dB.

Figure 5 shows the insertion losses corresponding to different aftertreatment muffler structures under medium and high frequency operating conditions (with the engine speed at 1800 rpm). For Scheme 1, a perforated baffle is added. By utilizing air viscous losses in the pores, the Helmholtz resonance effect, and acoustic scattering, the insertion loss for 3rd-order noise is increased by 0.5 dB, and that for the 6th-order noise by 0.3 dB. In Scheme 2, the imported perforated structure is further optimized for acoustic impedance matching, and the flow-acoustic coupling noise reduction is enhanced. As a result, the insertion losses at the 3rd and 6th orders are increased by 1.7 dB and 2.0 dB, respectively, compared with the original scheme, with an overall insertion loss improvement of 1.8 dB. This indicates that the suppression of broadband noise in the medium and high frequency range is gradually strengthened with successive iterations of the schemes.

At lower engine speed (600 rpm), the numerical results indicate that exhaust noise reduction is predominantly characterized by low-frequency and broad-spectrum attributes. The effectiveness of the perforated structure is therefore primarily attributed to low-frequency sound absorption mechanisms, including viscous dissipation and resonant absorption. This observation is consistent with classical engine noise theory, which attributes low-frequency exhaust noise mainly to engine order excitation [15].

Under high engine speed conditions (1800 rpm), noise energy shifts toward the medium and high frequency domains, and the noise reduction effect becomes increasingly dependent on enhanced mechanisms targeting these frequency ranges, such as flow-acoustic coupling and acoustic impedance modulation. Similar trends have been reported in previous studies on automotive exhaust systems, which indicate that flow-induced noise plays an increasingly significant role at higher flow velocities [16]. This further validates the rationale for classifying the operating conditions into low- and high-speed regimes.

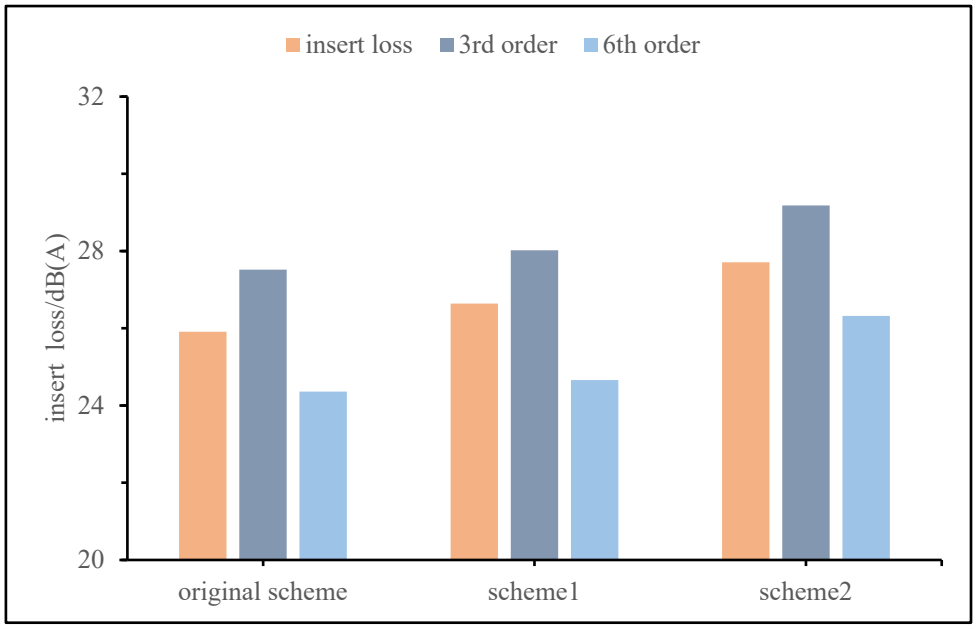

Figure 4. Insertion Loss at 600 rpm for Different Schemes.

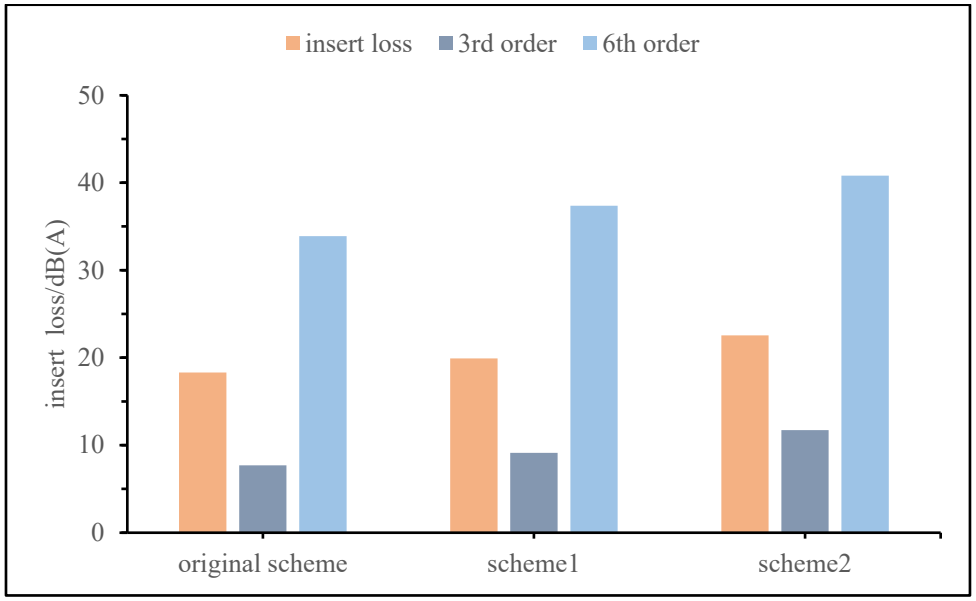

Figure 5. Insertion Loss at 1800 rpm for Different Schemes.

4.2. Experiment Results and Discussion

Figure 6 compares the vehicle pass-by noise results of different aftertreatment muffler structures at an engine speed of 600 rpm. The results values are reported as the mean of three repeated tests, with error bars representing the standard deviation (SD). In Scheme 1, a perforated baffle is added at the middle section of the flow channel to attenuate of sound propagation. Scheme 2, built upon Scheme 1, incorporates a perforated structure at the inlet to achieve pre-regulation of the flow field. The vehicle pass-by noise of Scheme 2 decreased by 0.9 dB compared with Scheme1. Similar studies [12] have reported that removing the inlet perforated structure led to an increase in insertion loss. This discrepancy may be related to differences in system configuration. In the present study, the inlet perforated structure serves as a flow-field pre-regulation element that suppresses flow-induced excitation, whereas in other configurations it may contribute additional noise.

For the 3rd-order noise, the maximum discrepancy among the three schemes is within 0.6 dB. This is attributed to the fact that the 3rd-order noise is dominated by rigid-body vibration excitation; its energy stems from structural imbalance in engine rigid-body motion. This behavior is consistent with classical exhaust noise theory [17], which indicates that low-order noise components are mainly governed by structure-borne excitation rather than in-duct acoustic or flow control mechanisms, thereby limiting the effectiveness of passive exhaust modifications for such orders. Neither Scheme 1 nor Scheme 2 can overcome the “shielding effect of structural excitation on the cross-domain mechanism”.

Results for the 6th-order noise demonstrate a dynamic balance between acoustic attenuation and flow-field regulation. Scheme 1 achieves a 17.3% reduction by directly attenuating in-pipe acoustic energy through Helmholtz resonance induced by the mid-channel perforated baffle, which is consistent with classical muffler behavior for mid-order tonal components [18]. Scheme 2, by contrast, intervenes upstream via its perforated inlet structure. The combined effect of flow field pre-regulation and acoustic transmission optimization ultimately results in superior overall noise performance.

The energy attenuation of the 9th-order noise is governed by high-frequency viscous losses and flow–acoustic interaction within the perforated baffle, while inlet flow-field pre-regulation further suppresses high-frequency flow-induced excitation. At such frequencies, perforated structures are known to be effective in dissipating high-order acoustic energy. This leads to converging attenuation amplitudes for Schemes 1 and 2.

Figure 7 shows the pass-by noise results at an engine speed of 650 rpm. Unlike the case at 600 rpm, distinct differences are observed in the 3rd-order noise among the schemes. As the engine speed increases, airflow turbulence intensifies, and Scheme 2 achieves an 8.0 dB reduction in the 3rd-order noise by effectively attenuating airflow pulsations through the inlet perforated structure. In contrast, Scheme 1 exhibits a slight increase in 3rd-order noise due to the absence of upstream flow-field intervention and the secondary excitation induced by the mid-channel structure. These findings indicate that, with increasing engine speed, the 3rd-order excitation undergoes a gradual transition from a rigidity-dominated to a flow-induced dominated regime. Under such conditions, the flow field pre-regulation mechanism of Scheme 2 exhibits a more pronounced inhibitory effect on flow-induced noise.

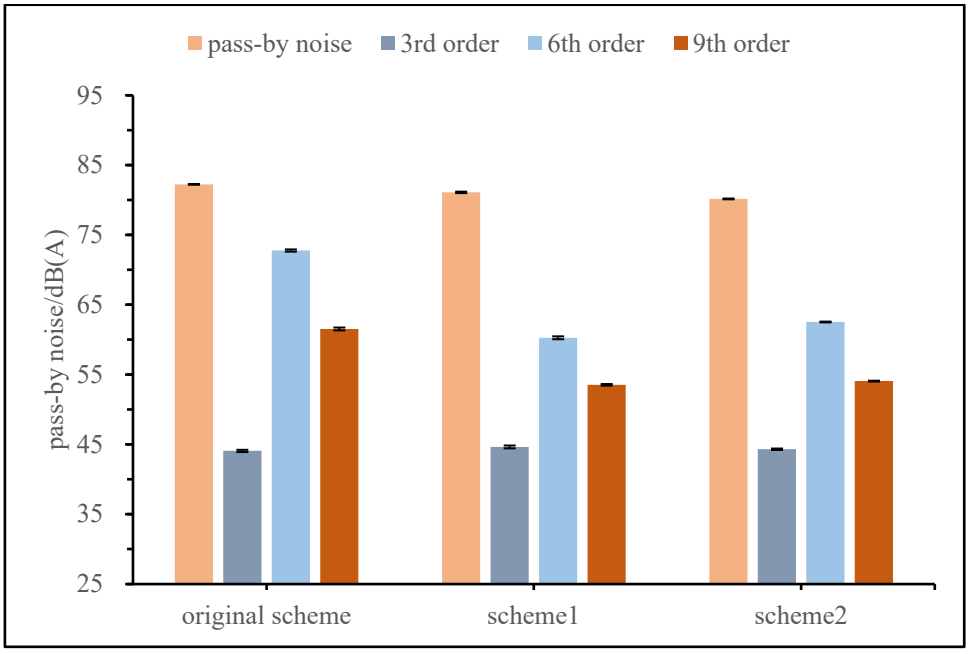

Figure 6. Pass-by Noise at 600 rpm for Different Schemes.

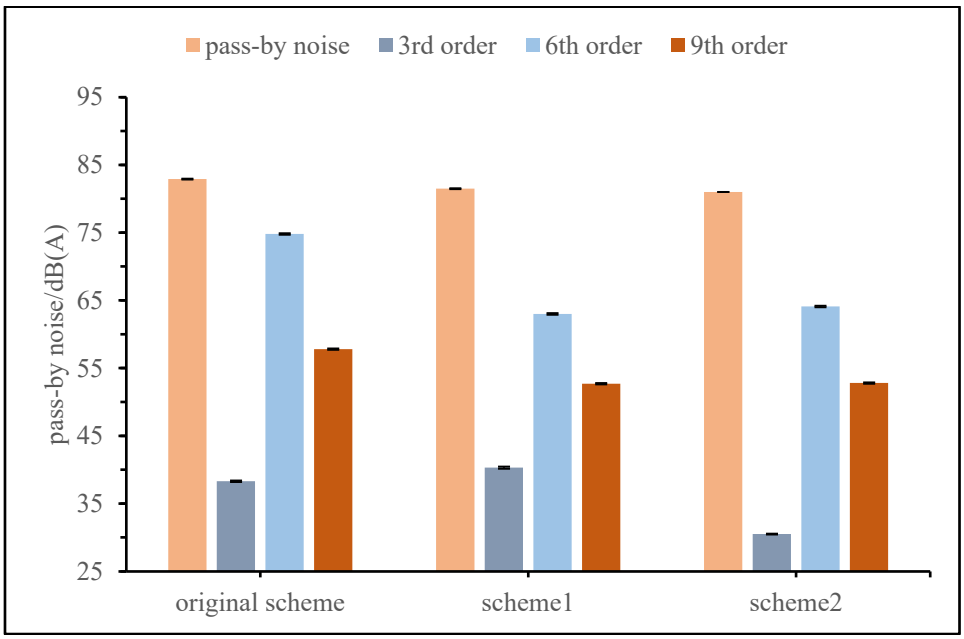

Figure 7. Pass-by Noise at 650 rpm for Different Schemes.

5. Conclusions

This paper optimizes two aftertreatment muffler structures using a combined simulation-experimental approach, thereby improving the exhaust noise performance. The main conclusions are as follows:

(1) Under low speed operating conditions (600 rpm), the exhaust noise exhibits low-frequency broadband characteristics, whereas at higher engine speed (1800 rpm), the noise energy shifts toward medium and high frequency range.

(2) At an engine speed of 600 rpm, the 3rd-order noise demonstrates strong insensitivity to mechanism-based interventions. This holds whether the muffler structure is modified by adding a perforated baffle alone or by combining a perforated baffle with an additional perforated structure at the inlet. A similar response is observed for the 9th-order noise, indicating limited effectiveness of both flow field pre-regulation and acoustic treatment inside the pipe under low-speed conditions.

(3) With a slight increase in engine speed from 600 rpm to 650 rpm, the dominant excitation mechanism of the 3rd-order noise shifts from rigidity-dominated excitation to flow-induced excitation, revealing a transition in the governing noise generation mechanism.

(4) The combined approach of adding a perforated baffle and incorporating a perforated structure at the inlet achieves superior overall noise reduction performance.

Author Contributions: M.C.: writing—original draft preparation and manuscript revision; C.X.: experimental work; J.L.: simulation and numerical calculations; W.Z. and P.L.: design and preparation of prototype samples; Z.C. and L.Z.: resource coordination; J.Z.: supervision and project administration. All authors have read and agreed to the published version of the manuscript.

Funding: This research received no external funding.

Data Availability Statement: Not applicable.

Conflicts of Interest: The authors declare no conflict of interest.

Use of AI and AI-Assisted Technologies: During the preparation of this work, the authors used Grammarly to optimize grammar checking and expression clarity of the text. After using this tool, the authors reviewed and edited the content as needed and take full responsibility for the content of the published article.

References

1. Munjal, M.L. Recent advances in muffler acoustics. *Int. J. Acoust. Vib.* **2013**, *18*, 71–85.
2. Bire, S.R.; Shelke, R.S. Review on design of resonating membrane type reactive muffler for IC engines. *Int. J. Adv. Res. Sci. Eng.* **2016**, *5*, 176–184.
3. Kashikar, R.; Suryawanshi, N.; Sonone, N.; Thorat, R.; Savant, S. Development of muffler design and its validation. *Appl. Acoust.* **2021**, *180*, 108132.
4. Sedighi, S.; Kalantari, D.; Rédl, J.; Kaveh, M.; Szymanek, M.; Dziwulska-Hunek, A. The effect of muffler design on reducing the noise pollution of a small two-stroke engine. *Results Eng.* **2024**, *23*, 101691.
5. Dong, Q.; Liu, X.; Qi, H.; Sun, C.; Wang, Y. Analysis and evaluation of electromagnetic vibration and noise in permanent magnet synchronous motor with rotor step skewing. *Sci. China Technol. Sci.* **2019**, *62*, 839–848.
6. Song, Z.; Liu, X.; Fang, Y.; Wang, X.; Su, S. Topology optimization for cold plate using neural networks as proxy models. *Eng. Optim.* **2024**, *56*, 2359–2386.
7. Guo, H.; Wang, Y.S.; Liu, N.N.; Yu, R.P.; Zhu, Z.G. Active interior noise control for rail vehicle using a variable step-size median-LMS algorithm. *Mech. Syst. Signal Process.* **2018**, *109*, 15–26.
8. Mohammad, M.; Muhamad Said, M.F.; Rajoo, S. Muffler internal geometry parametric study related to sound transmission loss and pressure drop. *J. Mek.* **2021**, *44*, 12–25.
9. Li, F.; Yuan, W.; Ma, Y.; Fu, J. Structural performance analysis and optimization of small diesel engine exhaust muffler. *Processes* **2024**, *12*, 2186.
10. Das, S.; Mondal (Das), K.; Ahmad, A.; Ali, S.S.; Faizan, M.; Ameen, S.; Pandey, A.; Vadiraja, B.R. A novel design for muffler chambers by incorporating baffle plate. *Appl. Acoust.* **2022**, *197*, 108888.
11. Huang, P.; Wu, P.; Su, H.; Xue, J.; Zhang, H.; Zhang, Y.; Guo, Y. Research on the acoustic attenuation performance and optimization of split-stream rushing exhaust mufflers in the presence of acoustic–structure coupling effects. *Appl. Sci.* **2025**, *15*, 4722.
12. Duan, J.; Zhang, X.; Lu, C.; Xu, S.; Zhou, S.; Li, F. Research on the Noise of the Engine Exhaust System. *Int. Combust. Eng. Parts* **2022**, *5*, 4–7.
13. Zheng, Z. Acoustical Research and Design of Diesel Engine Exhaust System in CN VI Standard. Master's Thesis, Nanjing University of Aeronautics and Astronautics, Nanjing, China, 2018.
14. Li, L. The Research on the Noise Reduction of the Engine Exhaust System. *Small Int. Combust. Eng. Veh. Tech.* **2020**, *49*, 79–84.
15. Heywood, J.B. *Internal Combustion Engine Fundamentals*; McGraw-Hill: New York, NY, USA, 1988.
16. Selamet, A.; Dickey, N.S.; Novak, J.M. Flow-induced noise mechanisms in automotive exhaust mufflers. *Appl. Acoust.* **2005**, *66*, 673–699.
17. Munjal, M.L. *Acoustics of Ducts and Mufflers*; John Wiley & Sons: New York, NY, USA, 2014.
18. Selamet, A.; Radavich, P.M. Acoustic attenuation performance of perforated tube mufflers. *J. Sound Vib.* **1997**, *201*, 407–426.